Conventional Profile Coaxial Jet Noise Prediction

James R. Stone,* Donald E. Groesbeck,† and Charles L. Zola‡
NASA Lewis Research Center, Cleveland, Ohio

A semiempirical model for predicting the noise generated by conventional velocity-profile jets exhausting from coaxial nozzles is presented and compared with small-scale static data. The present method is an updated version of that part of the original NASA Aircraft Noise Prediction Program (1974) relating to coaxial jet noise. The new procedure is more theoretically based and has also been improved by some empirical adjustments.

Nomenclature

A = area
c = speed of sound
D = nozzle hydraulic diameter
F = functional relation, Eq. (4)
F_S = frequency shift parameter defined in Eq. (3)
f = center frequency, one-third octave band
M = Mach number, V/c
m = exponent defined in Eq. (2)
OASPL = overall sound pressure level, dB (20 μN/m^2)
p = pressure
R = source-to-observer distance
S = effective Strouhal number
SPL = sound pressure level, one-third octave band, dB (20 μN/m^2)
T = total temperature
UOL = predicted OASPL uncorrected for refraction, dB (20 μN/m^2)
V = velocity
Y = minimum (perpendicular) distance of observer from engine axis (Fig. 1), deg
α = jet angle of attack (Fig. 1), deg
ρ = density
θ = polar angle from inlet axis (Fig. 1), deg
θ' = effective polar angle, $\theta(V_j/c_a)^{0.1}$, deg
θ_M = Mach angle, 180 deg $-\sin^{-1}(1/M_j)$, deg
ϕ = azimuthal angle (Fig. 1), deg
ψ = modified (aircraft) directivity angle (Fig. 1), deg
ω = density exponent, Eq. (A1b)

Subscripts

a = ambient or apparent
c = convection
e = effective
ISA = international standard atmosphere (288 K and 101.3 kN/m^2)
j = fully expanded jet
s = shock noise
90° = parameter evaluated at $\theta = 90$ deg
0 = aircraft
1 = fully expanded primary (inner) jet
2 = fully expanded secondary (outer) jet

Introduction

ALTHOUGH the numerous aspects of the mechanisms of noise generation by coaxial jets are not fully understood, the necessity of predicting jet noise has led to the development of empirical procedures. The NASA interim prediction method for jet noise[1] and several different methods based on extension of the Society of Automotive Engineers (SAE) method for circular jets[2] are in current use. The NASA interim method has already been shown to agree reasonably well with model and full-scale static and flight data[3] for coaxial jets having low to moderately high bypass ratios. The circular jet method has since been improved by incorporating a more theoretically justified formulation of source convection effects.[4] It is appropriate, furthermore, to incorporate the improved convection formulation[4] in the conventional velocity-profile coaxial jet mixing noise prediction procedure, along with the empirical improvements motivated by the comparisons of Ref. 5 and some minor changes in the treatment of flight effects. For the case of supersonic primary (inner stream) and/or secondary (outer stream) jets, broadband shock/turbulence interaction noise is predicted by an extension of the semiempirical method developed for circular jets by Harper-Bourne and Fisher.[6]

The formulations of these predictions for jet mixing and shock noise are presented in this paper. The validity of these improved predictions is established by fairly extensive comparisons with model-scale static data. Because sufficient appropriate simulated-flight data are not available in the literature, verification of flight effects must be deferred.

Formulation of Procedure

The output of this prediction procedure is an array of SPL spectra at each angle of interest. (Acoustic power relations are not given explicitly, but power computations may be made by integrating the results numerically over all angles.) The jet mixing noise and shock noise are assumed to be symmetric

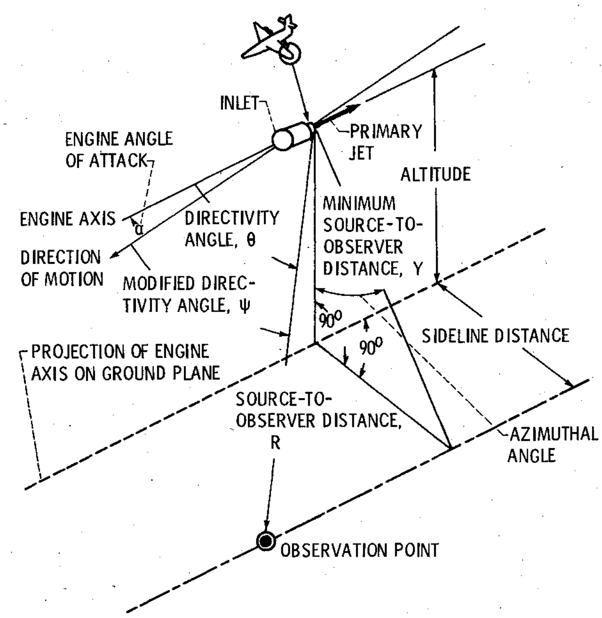

Fig. 1 Geometric variables describing position of airplane noise source with respect to an observation point.

Presented as Paper 81-1991 at the AIAA Seventh Aeroacoustics Conference, Palo Alto, Calif., Oct. 5-7, 1981; submitted Oct. 28, 1981; revision received July 12, 1982. This paper is declared a work of the U.S. Government and therefore is in the public domain.

*Head, Section A, Jet Acoustics Branch. Member AIAA.
†Research Engineer, Section A, Jet Acoustics Branch.
‡Research Engineer, Mission Analysis Office. Member AIAA.

about the jet axis. The geometric variables describing the position of the observer relative to the engine are shown schematically in Fig. 1. The noise levels predicted are free field (no reflections), far field, and lossless (i.e., the effects of atmospheric absorption are not included).

Jet Mixing Noise

Olsen and Friedman[7] correlated shock-free cold-flow coaxial jet noise data for a wide range of conditions based on an extension and modification of the method of Williams et al.[8] The method of Ref. 7 is modified and extended to account for the case of a heated, shock-free primary jet.

UOL

The effects of area ratio, velocity ratio, and temperature ratio on the OASPL uncorrected for refraction (UOL) relative to that of the isolated primary jet (UOL_1) is given by,

$$UOL - UOL_1 = 5\log\left(\frac{T_1}{T_2}\right) + 10\log\left[\left(1-\frac{V_2}{V_1}\right)^m + 1.2\frac{[1+(A_2V_2^2/A_1V_1^2)]^4}{[1+(A_2/A_1)]^3}\right] \tag{1}$$

In Eq. (1), UOL_1 is the OASPL uncorrected for refraction for the isolated primary jet calculated from the relations given in the Appendix, which is based on Ref. 4. The exponent m is

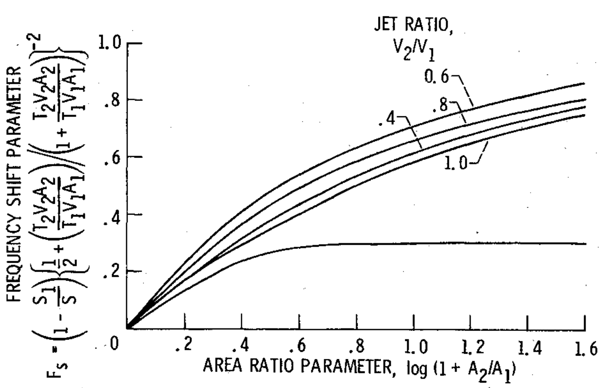

Fig. 2 Recommended frequency shift parameter for coaxial jets with respect to isolated primary jet, based on extension of the method of Olsen and Friedman.[7]

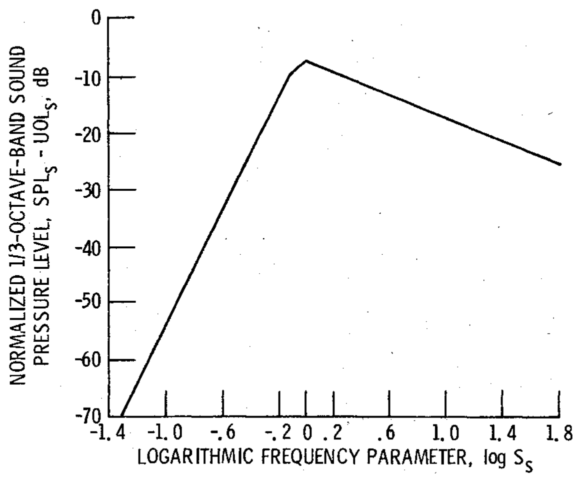

Fig. 3 Recommended one-third octave band spectrum for shock noise.[4]

Table 1 Recommended spectra for jet mixing noise

Frequency parameter, log S	Corrected directivity angle (referred to inlet), $\theta' = \theta(V_j/c_a)^{0.1}$, deg; Normalized sound pressure level, SPL – UOL, dB: 0-110	120	130	140	150	160	170	180	190	200	250
-3.6	-85.0	-90.0	-95.0	-100.0	-100.0	-100.0	-100.0	-90.0	-80.0	-70.0	-60.0
-1.8	-40.5	-40.4	-40.4	-40.3	-40.1	-39.5	-37.5	-36.0	-35.0	-34.0	-33.8
-1.7	-38.0	-37.8	-37.4	-37.1	-37.0	-36.4	-33.5	-33.0	-32.5	-32.0	-32.0
-1.6	-35.6	-35.4	-34.4	-33.8	-33.5	-33.3	-30.0	-30.0	-30.0	-30.0	-31.0
-1.5	-33.3	-33.2	-31.4	-30.3	-30.0	-29.5	-27.0	-27.0	-27.5	-28.0	-30.0
-1.4	-30.9	-30.9	-28.5	-26.8	-26.4	-25.5	-24.5	-25.0	-25.5	-26.0	-31.0
-1.3	-28.6	-28.6	-25.7	-23.4	-23.0	-22.8	-22.5	-23.0	-23.5	-24.0	-32.5
-1.2	-26.2	-26.2	-22.9	-19.8	-19.4	-20.0	-20.5	-21.0	-21.5	-22.0	-34.5
-1.1	-24.0	-24.0	-20.1	-16.2	-16.8	-17.5	-18.5	-19.0	-19.5	-20.0	-36.6
-1.0	-21.8	-21.8	-17.3	-13.2	-14.5	-16.2	-16.5	-17.0	-17.5	-18.5	-38.8
-.9	-19.5	-19.5	-14.7	-11.2	-13.1	-14.7	-15.5	-16.0	-17.0	-19.0	-40.1
-.8	-17.5	-17.4	-13.0	-10.2	-11.0	-13.5	-14.5	-15.5	-17.5	-20.0	-42.5
-.7	-15.9	-15.6	-11.5	-9.5	-9.4	-12.6	-14.0	-16.5	-18.5	-21.0	-45.0
-.6	-14.7	-14.0	-9.7	-8.8	-8.3	-12.0	-14.5	-18.0	-20.0	-22.0	-47.5
-.5	-13.7	-12.4	-9.0	-8.1	-7.7	-11.7	-15.8	-20.0	-21.8	-23.5	-50.0
-.4	-12.8	-11.0	-8.9	-8.4	-8.3	-12.6	-17.9	-22.2	-24.1	-25.9	-52.5
-.3	-12.1	-10.2	-9.1	-8.9	-9.8	-14.5	-20.0	-24.4	-26.4	-28.3	-55.0
-.2	-11.6	-9.9	-9.6	-9.8	-11.6	-16.4	-22.1	-26.6	-28.7	-30.7	-57.5
-.1	-11.3	-10.2	-10.8	-11.3	-13.4	-18.3	-24.2	-28.8	-31.0	-33.1	-60.0
.0	-11.1	-10.6	-12.0	-12.9	-15.2	-20.2	-26.3	-31.0	-33.3	-35.5	-62.5
+.1	-11.2	-11.1	-13.3	-14.5	-17.0	-22.1	-28.4	-33.2	-35.6	-37.9	-65.0
.2	-11.3	-11.8	-14.6	-16.1	-18.8	-24.0	-30.5	-35.4	-37.9	-40.3	-67.5
.3	-11.7	-12.7	-15.9	-17.7	-20.6	-25.9	-32.6	-37.6	-40.2	-42.7	-70.0
.4	-12.3	-13.7	-17.2	-19.3	-22.4	-27.8	-34.7	-39.8	-42.5	-45.1	-72.5
.5	-13.0	-14.7	-18.5	-20.9	-24.2	-29.7	-36.8	-42.0	-44.8	-47.5	-75.0
.6	-13.7	-15.8	-19.8	-22.5	-26.0	-31.6	-38.9	-44.2	-47.1	-49.9	-77.5
.7	-14.6	-16.9	-21.1	-24.1	-27.8	-33.5	-41.0	-46.4	-49.4	-52.3	-80.0
.8	-15.6	-18.0	-22.4	-25.7	-29.6	-35.4	-43.1	-48.6	-51.7	-54.7	-82.5
.9	-16.7	-19.2	-23.7	-27.3	-31.4	-37.3	-45.2	-50.8	-54.0	-57.1	-85.0
1.0	-17.8	-20.4	-25.0	-28.9	-33.2	-39.2	-47.3	-53.0	-56.3	-59.5	-87.5
1.1	-18.9	-21.6	-26.3	-30.5	-35.0	-41.1	-49.4	-55.2	-58.6	-61.9	-90.0
1.2	-20.1	-22.8	-27.6	-32.1	-36.8	-43.0	-51.5	-57.4	-60.9	-64.3	-92.5
1.3	-21.3	-24.0	-28.9	-33.7	-38.6	-44.9	-53.6	-59.6	-63.2	-66.7	-95.0
1.4	-22.4	-25.2	-30.2	-35.3	-40.4	-46.8	-55.7	-61.8	-65.5	-69.1	-97.5
1.5	-23.6	-26.4	-31.5	-36.9	-42.2	-48.7	-57.8	-64.0	-67.8	-71.5	-100.0
1.6	-24.8	-27.6	-32.8	-38.5	-44.0	-50.6	-59.9	-65.2	-70.1	-73.9	-102.5
1.7	-26.0	-28.8	-34.1	-40.1	-45.8	-52.5	-62.0	-68.4	-72.4	-76.3	-105.0
1.8	-27.2	-30.0	-35.4	-41.7	-47.6	-54.4	-64.1	-70.6	-74.7	-78.7	-107.5
3.6	-48.8	-51.6	-58.8	-70.5	-80.0	-88.6	-101.9	-110.2	-116.1	-121.9	-152.5
OASPL–UOL	.0	+.1	+.5	+1.1	+.4	-3.2	-5.8	-7.7	-9.0	-10.6	

given by

$$m = 1.1\sqrt{A_2/A_1}; \quad A_2/A_1 < 29.7$$
$$= 6.0; \quad A_2/A_1 \geq 29.7 \tag{2}$$

Spectra

The shapes of the SPL spectra for shock-free coaxial jets were generally found to be similar to those of the isolated primary jet, but with the peak frequency shifted.[7] In Fig. 2 the effect of area ratio and velocity ratio on the frequency shift parameter F_S is shown, where

$$F_S = \left(1 - \frac{S_1}{S}\right)\left[\frac{1}{2} + \frac{T_2V_2A_2/T_1V_1A_1}{1 + (T_2V_2A_2/T_1V_1A_1)}\right]^{-2} \tag{3}$$

In Eq. (3), S_1 is the effective Strouhal number for the isolated primary nozzle calculated from the Appendix. From Eq. (3) and Fig. 2, the nondimensionalized frequency ratio (coaxial to isolated primary) S/S_1 can be calculated, which gives the frequency shift relative to the isolated primary nozzle. The SPL(f) can then be obtained from Table 1.

OASPL

The overall sound pressure level is obtained by integrating the spectral results over the frequency range of interest.

Shock Noise

The shock noise, for each stream which is supersonic, is calculated separately. It is assumed that there is no interaction between the two streams. This method was evolved from the model of Harper-Bourne and Fisher[6] and the experimental results of Seiner and Norum.[9] The overall sound pressure level uncorrected for refraction, for either stream which is supersonic, $\mathrm{UOL}_{s,j}$, is given by

$$\mathrm{UOL}_{s,j} = 162 + 10\log\left[\left(\frac{\rho_a}{\rho_{\mathrm{ISA}}}\right)^2\left(\frac{c_a}{c_{\mathrm{ISA}}}\right)^4\right] + 10\log\left(\frac{A_j}{R^2}\right) + 10\log\left[\frac{(M_j^2-1)^2}{1+(M_j^2-1)^2}\right] - 10\log[1 - M_0\cos\psi] + F(\theta - \theta_M) \tag{4a}$$

where ψ is the angle of the observer relative to the direction of aircraft motion, the Mach angle is given by $\theta_M = 180$ deg $- \sin^{-1}(1/M_j)$, and the subscript $j=1$ refers to the primary (inner) stream and $j=2$ to the secondary (outer) stream. The function F is given by

$$F = 0 \quad \text{for } \theta \leq \theta_M$$
$$= -0.75 \quad \text{for } \theta > \theta_M \tag{4b}$$

The appropriate nondimensional frequency parameter is given by

$$S_{s,j} = \left(\frac{fD_j}{0.7V_j}\right)\sqrt{M_j^2 - 1}\,(1 - M_0\cos\psi) \times \sqrt{\left[1 + 0.7\left(\frac{V_j}{c_a}\right)\cos\theta\right]^2 + 0.0196\left(\frac{V_j}{c_a}\right)^2} \tag{5}$$

where D_j is the hydraulic diameter. Note that the convection velocity factor is 0.7 instead of the 0.62 value used for jet mixing noise, but that the 0.2 value of the turbulent length scale ratio is retained, which leads to the 0.0196 factor. The shock noise peaks at $S_{s,j} = 1.0$ and varies with $\log S_{s,j}$ as shown in Fig. 3. The $\mathrm{SPL}_{s,j}$ as a function of frequency is then determined from Fig. 3, where $S_{s,j}(f)$ is obtained from Eq.

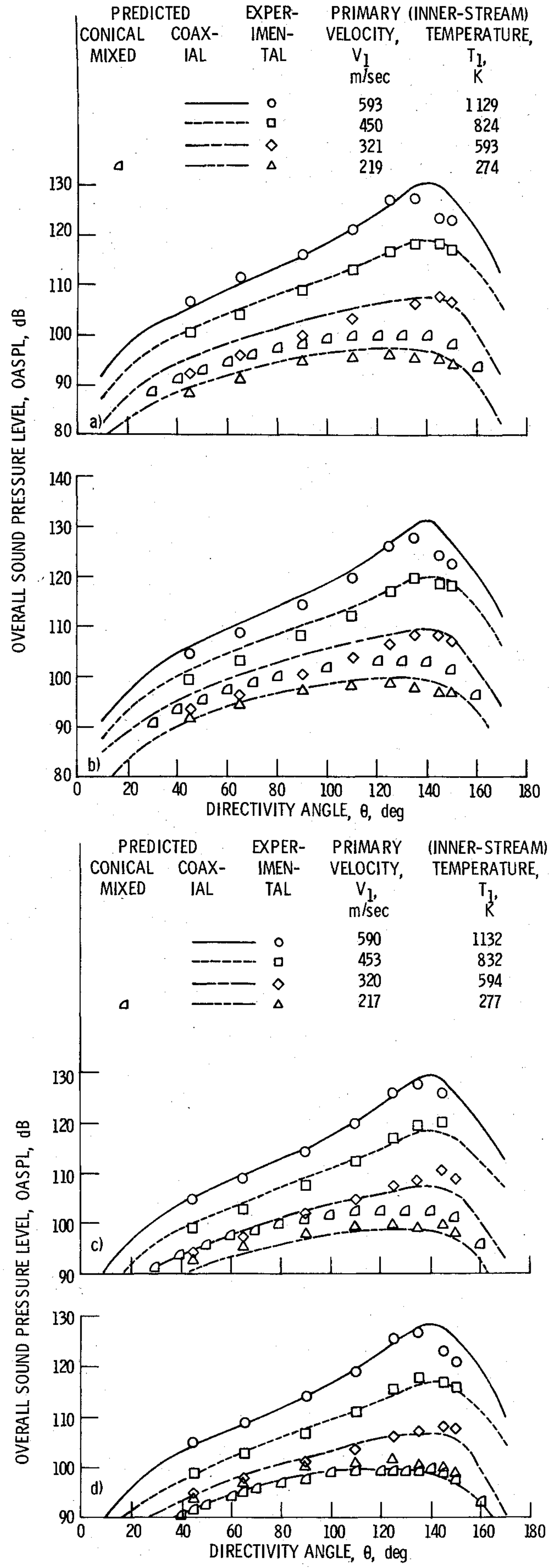

Fig. 4 Comparison of predicted and experimental effect of primary conditions on lossless free-field OASPL directivity on 5.0 m sideline (secondary velocity $V_2 \simeq 215$ m/s, temperature $T_2 \simeq 279$ K); area ratio A_2/A_1 equals: a) 1.2, noncoplanar; b) 1.4, coplanar; c) 1.9, coplanar; d) 3.2, coplanar.

(5). Some effects of jet temperature and directivity angle on spectral shape and level have been observed by von Glahn[10] and others for circular jets; perhaps such effects are also applicable to coaxial jets, but they are not presently included. Shock noise is not projected to be a factor for future high-bypass engines, since both jet stream conditions are subsonic at takeoff and landing.

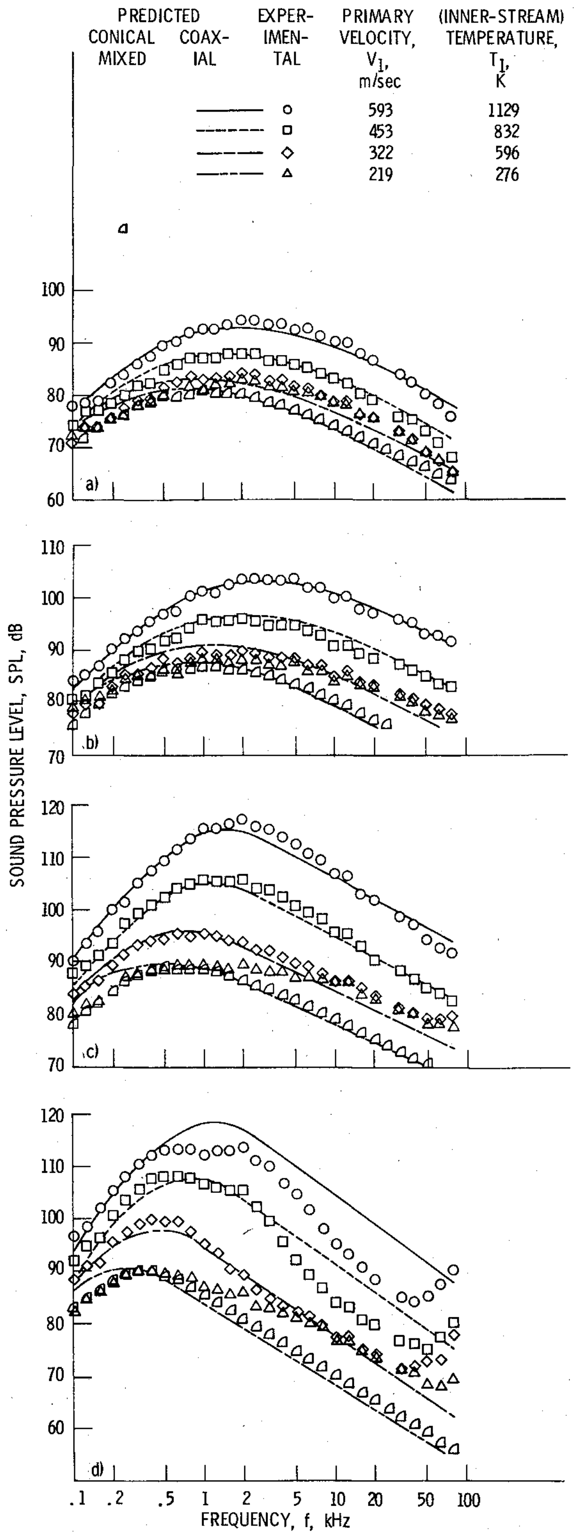

Fig. 5 Comparison of predicted and experimental effect of primary velocity and temperature on lossless free-field subsonic spectra at 5.0 m sideline (3.2 area ratio coaxial coplanar nozzle, 10 cm primary nozzle diameter, secondary velocity $V_2 \approx 216$ m/s, temperature $T_2 \approx 280$ K), directivity angle θ equals: a) 45 deg, b) 90 deg, c) 125 deg, d) 145 deg.

Comparisons with Experimental Data

This section contains limited comparisons of the present prediction method with experimental data for model coaxial jets. Although there exists a great deal of additional experimental data with which comparisons may eventually be made, the present comparisons are considered to be sufficient to demonstrate the validity of the procedure. Comparisons with conical nozzle data are presented in the Appendix to illustrate the validity of the conical nozzle basis for the present method.

Static Jet Mixing Noise

Multiple sideline jet noise measurements were obtained by Goodykoontz et al.[11] for a series of four coaxial nozzles having secondary-to-primary area ratios A_2/A_1 of 1.2-3.2 and a common primary nozzle diameter of 10.0 cm. These data are corrected for source position by the method of Ref. 4.

OASPL

Sideline directivity patterns for each nozzle configuration are shown in Fig. 4. In each case, the secondary conditions are held essentially constant at $V_2 \approx 215$ m/s and $T_2 \approx 279$ K, and the primary conditions are varied widely. It can be seen that the prediction method is reasonably accurate in predicting the noise directivity for this wide range of inner-stream conditions. It can also be seen, by comparing the results for the various configurations, that the effects of area ratio and of noncoplanar exits are predicted reasonably well. It is also significant that the prediction method produces proper limiting results as the velocity ratio V_2/V_1 and temperature ratio T_2/T_1 approach unity. Not only does the present prediction agree with the experimental data in this limiting case, but it agrees better with these data than does the noise predicted (see Appendix) for a single-stream circular nozzle operating at the equivalent mixed-flow conditions (velocity, temperature, and mass flow rate). The standard deviation of the prediction method with respect to this data set is 1.8 dB and the average overprediction is 0.5 dB. Data for the other sideline distances (not shown) show similar agreement.

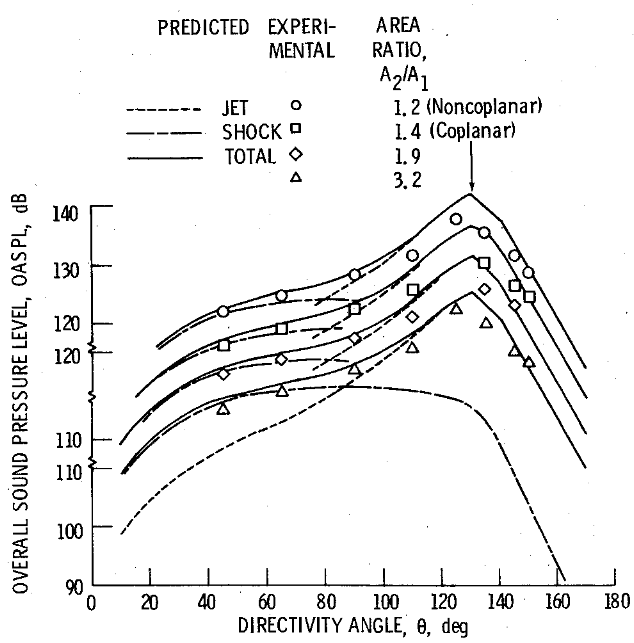

Fig. 6 Comparison of predicted and experimental effect of area ratio on supersonic jet mixing and shock noise lossless free-field OASPL directivity on 5.0 m sideline (high primary Mach number $M_1 \approx 1.38$, high primary velocity $V_1 \approx 790$ m/s, $T_1 \approx 1130$ K, 10 cm primary nozzle diameter, secondary velocity $V_2 \approx 216$ m/s, temperature $T_2 \approx 278$ K. (Data from Ref. 11.)

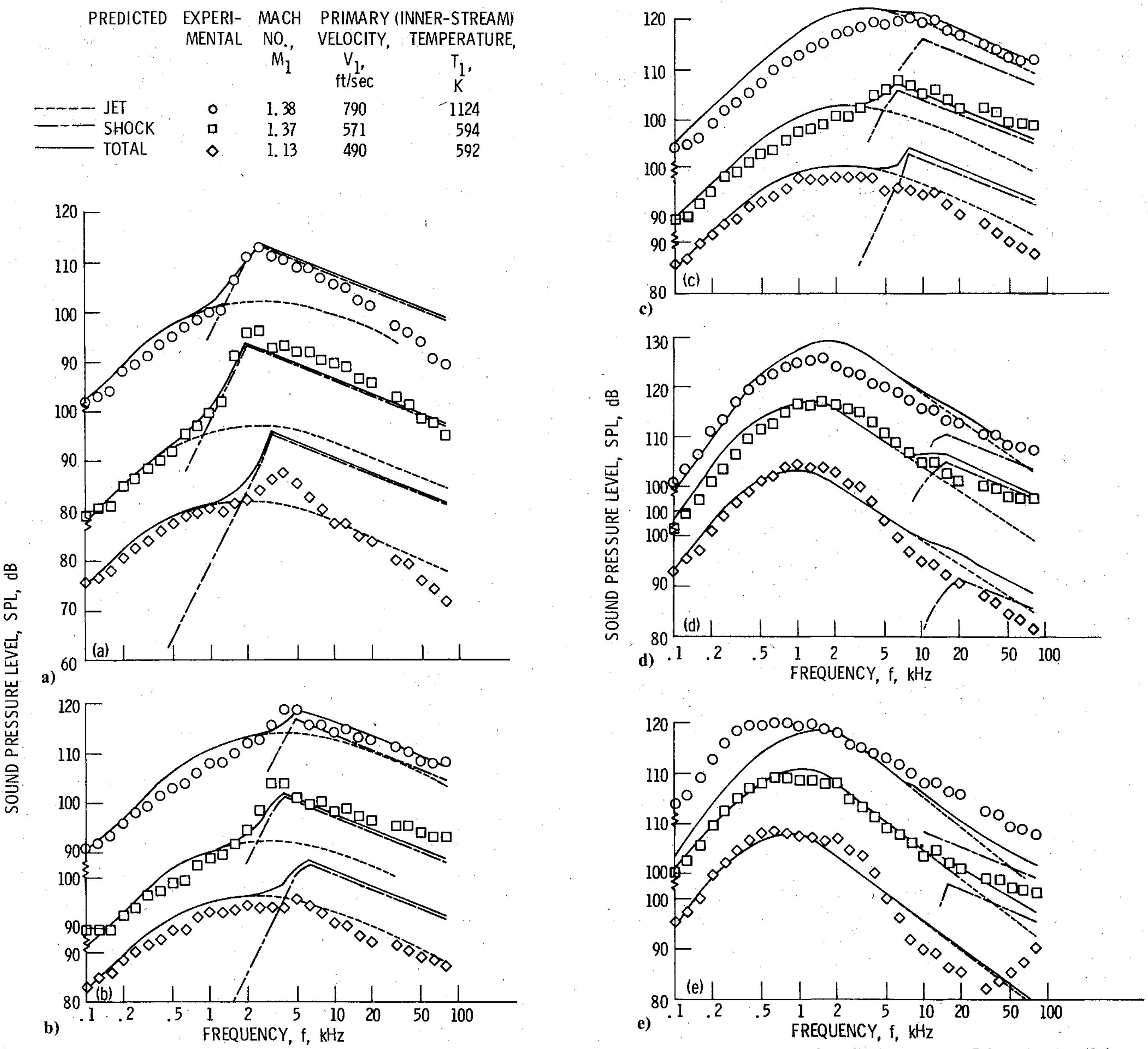

Fig. 7 Comparison of predicted and experimental effect of supersonic primary conditions on lossless free-field spectra at 5.0 m sideline (3.2 area ratio coaxial coplanar nozzle, 10 cm primary nozzle diameter, secondary velocity $V_2 \simeq 216$ m/s, temperature $T_2 \simeq 280$ K), directivity angle θ equals: a) 45 deg, b) 90 deg, c) 110 deg, d) 135 deg, e) 150 deg.

Spectra

Spectral comparisons for these same conditions are shown in Fig. 5 for an area ratio of 3.2 at directivity angles of 45, 90, 125, and 145 deg. Generally the agreement is good except at high frequencies near the jet axis, where there is an apparently anomalous reversal of slope which is worse at large propagation distances. This accentuation of anomalous behavior at large distances is not unexpected, since at large distances the corrections for atmospheric attenuation are large and nonlinear propagation effects might become important. These discrepancies were much less, even for large θ, for the closer sideline data (not shown). There is some tendency to overpredict the low-frequency noise and underpredict the high-frequency noise for the case where the conditions of the two streams approach equality. This problem is not a major one however, since the integrated measure, overall sound pressure level is reasonably accurate, and this is not a case of interest for real engine cycles.

Shock Noise

While shock noise is not likely to be a significant factor for future high-bypass engines, it should be included for generality and for the predictions of the noise for older, lower bypass engines and possible future supersonic transport engines. Therefore, limited directivity and spectral comparisons with the static experimental results of Ref. 11 at supersonic primary conditions are included.

OASPL

Sideline directivity patterns are shown in Fig. 6 for a fully expanded primary Mach number M_1 of 1.4 and primary temperature T_1 of 1130 K, producing a primary jet velocity V_1 of 790 m/s. The secondary conditions are held essentially constant at $V_2 \simeq 216$ m/s and $T_2 \simeq 278$ K. The predicted shock noise is indicated by the dash-dot curve, predicted jet mixing noise by the dashed curve and the total predicted noise by the solid curve. These comparisons at high Mach number indicate not only that the level of shock noise is predicted reasonably well, but that the mixing noise levels are predicted reasonably well even in the presence of shocks in the flowfield.

Spectra

Spectral comparisons for these same conditions are shown in Fig. 7 for the 3.2 area ratio nozzle along with data at different primary conditions. At the high Mach number, it appears that the shock noise is predicted reasonably accurately, and comparisons at the smaller area ratios (not shown) are consistent with these results. Especially for the large area ratio shown, the shock noise at low Mach number is overpredicted. This very well could be due to the large mass flow of the secondary impinging on the primary, causing an effectively lower primary pressure ratio and Mach number. Perhaps the most important result of these comparisons is that the jet mixing noise prediction validity is demonstrated to an inner-stream jet velocity of at least 790 m/s.

Conclusion

An improved semiempirical model for predicting the noise generated by jets exhausting from coaxial nozzles with conventional velocity profiles is presented and compared with small-scale static data. The prediction of jet mixing noise is based on the extensive experimental study and empirical correlation of Olsen and Friedman[7] for the effect of the secondary (outer-stream) relative to the isolated primary (inner-stream) jet. The isolated primary prediction used as a base is an improved NASA method for conical nozzles.[4] The effect of a primary nozzle plug is included in the prediction, but is not validated in the present paper. The shock noise for a supersonic primary or secondary is calculated from a model based on extension of the method of Harper-Bourne and Fisher.[6] The predictions formulated for both sources cover the full angular range of 0-180 deg. There are no inherent limitations on the range of the prediction methods, and comparisons with static model data are presented for primary jet velocities of 200-795 m/s. These comparisons indicate that the overall sound pressure level is predicted within a standard deviation of 1.8 dB.

Appendix: Single-Stream Jet Mixing Noise Prediction

Formulation

The coaxial jet noise prediction presented herein uses the noise of the hypothetical isolated primary jet as a building block. This Appendix presents these primary jet relationships, which are based on Ref. 4, with minor improvements and with the addition of plug nozzle effect from Ref. 1. The overall sound pressure level, without correction for refraction, UOL_1, is given by

$$\mathrm{UOL}_1 = 141 + 10\log\left[\left(\frac{\rho_a}{\rho_{\mathrm{ISA}}}\right)^2\left(\frac{c_a}{c_{\mathrm{ISA}}}\right)^4\right] + 10\log\left(\frac{A_1}{R^2}\right)$$

$$+10\log\left(\frac{\rho_1}{\rho_a}\right)^{\omega} + 10\log\left(\frac{V_e}{c_a}\right)^{7.5}$$

$$-15\log\left[(1+M_c\cos\theta)^2 + 0.04M_c^2\right]$$

$$-10\log[1-M_0\cos\psi] + 3\log\left(\frac{2A_1}{\pi D_1^2}+\frac{1}{2}\right) \qquad \text{(A1a)}$$

where

$$V_e = V_1\left[1-(V_0/V_1)\cos\alpha\right]^{2/3} \qquad \text{(A1b)}$$

$$\omega = \frac{3(V_e/c_a)^{3.5}}{0.6+(V_e/c_a)^{3.5}} - 1 \qquad \text{(A1c)}$$

$$M_c = 0.62(V_1 - V_0\cos\alpha)/c_a \qquad \text{(A1d)}$$

The modified directivity angle ψ is the angle of the observer relative to the direction of aircraft motion. The angle of attack α is the angle of the upstream axis of the jet relative to the direction of aircraft motion. For flyover directly over the observer, $\psi = \theta - \alpha$. Spectral relationships are given in Table 1,

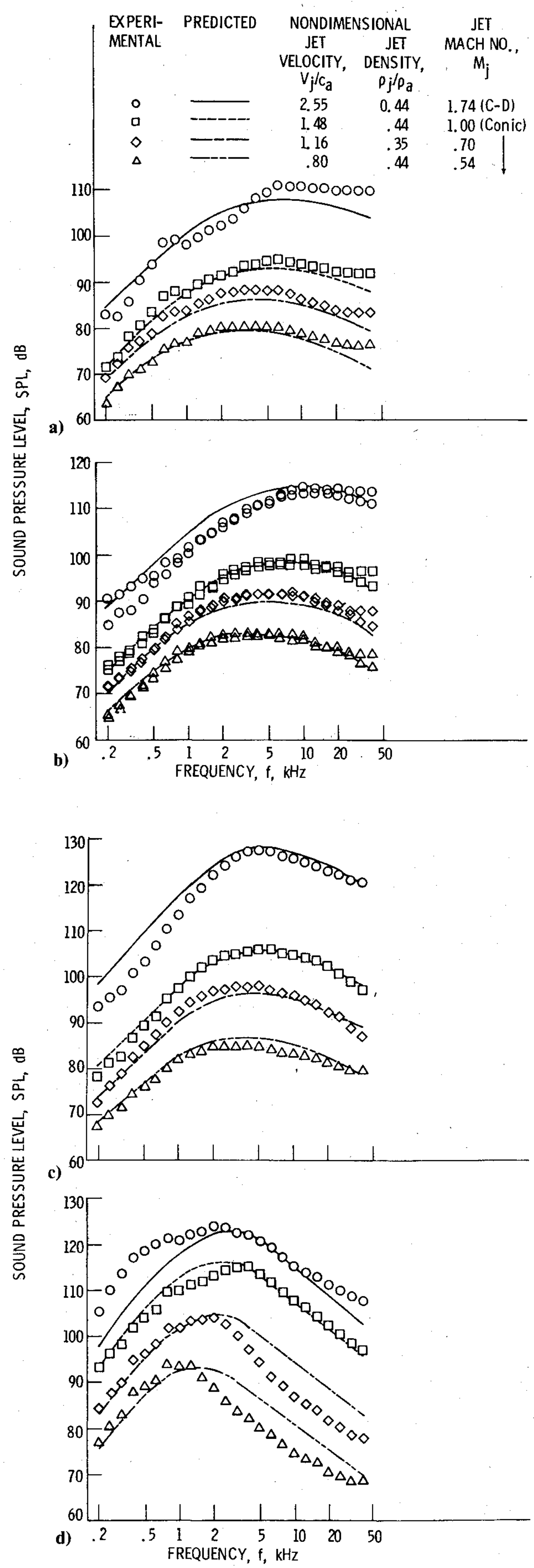

Fig. A1 Comparison of predicted and experimental effect of single-stream jet conditions on lossless free-field shock-free spectra on a 3.66 m arc (experimental data of Tanna et al.[12] for 5.08 cm diam conical and circular convergent-divergent nozzles), directivity angle θ equals: a) 57 deg, b) 86 deg, c) 116 deg, d) 155 deg.

where SPL − UOL is given at various corrected angles, $\theta' = \theta(V_I/c_a)^{0.1}$ as a function of the logarithm of the effective Strouhal number S. For the single stream case, $S = S_I$, where

$$S_I = \frac{f\sqrt{4A_I/\pi}}{V_e}\left(\frac{D_I}{\sqrt{4A_I/\pi}}\right)^{0.4}\left(\frac{T_I}{T_a}\right)^{0.4(1+\cos\theta')}[1 - M_0\cos\psi]$$

$$\times\left\{\left[1+0.62\left(\frac{V_I-V_0}{c_a}\right)\cos\theta\right]^2+0.01538\left(\frac{V_I-V_0}{c_a}\right)^2\right\}^{1/2}$$

$$\div\left\{\left[1+0.62\left(\frac{V_I}{c_a}\right)\cos\theta\right]^2+0.01538\left(\frac{V_I}{c_a}\right)^2\right\}^{1/2} \quad \text{(A2)}$$

Table 1 differs somewhat from that given in Ref. 4, in order to produce a more accurate prediction at the peak noise angle and near the jet axis, based on the comparisons of Gutierrez.[5]

Validation

Since minor improvements have been made with respect to Ref. 4, some of the comparisons shown therein with the data of Tanna et al.[12] are repeated here using the modified prediction. In Fig. A1 spectral comparisons with the data of Ref. 12 are shown at directivity angles of 57, 86, 116, and 155 deg for jet velocities of 0.8-2.55 times the ambient sonic velocity. The agreement is reasonably good.

References

[1] Stone, J. R., "Interim Prediction Method for Jet Noise," NASA TM X-71618, 1974.

[2] "Gas Turbine Jet Exhaust Noise Prediction," SAE ARP-876, March 1978.

[3] Stone, J. R., "Prediction of In-Flight Exhaust Noise for Turbojet and Turbofan Engines," *Noise Control Engineering*, Vol. 10, Jan.-Feb. 1978, pp. 40-46.

[4] Stone, J. R. and Montegani, F. J., "An Improved Prediction Method for the Noise Generated in Flight by Circular Jets," NASA TM-81470, 1980.

[5] Gutierrez, O. A., "Effect of Facility Variation on the Acoustic Characteristics of Three Single Stream Nozzles," NASA TM-81635, 1980.

[6] Harper-Bourne, M. and Fisher, M. J., "The Noise from Shock Waves in Supersonic Jets," Advisory Group for Aerospace Research and Development, *Noise Mechanisms*, AGARD-CP-131, 1973, pp. 11-1-11-13.

[7] Olsen, W. A. and Friedman, R., "Jet Noise from Coaxial Nozzles over a Wide Range of Geometric and Flow Parameters," AIAA Paper 74-43, Jan. 1974.

[8] Williams, T. J., Ali, M.R.M.H., and Anderson, J. S., "Noise and Flow Characteristics of Coaxial Jets," *Journal of Mechanical Engineering Science*, Vol. 11, April 1969, pp. 133-142.

[9] Seiner, J. M. and Norum, T. D., "Experiments on Shock Associated Noise of Supersonic Jets," AIAA Paper 79-1526, July 1979.

[10] von Glahn, U., "New Interpretations of Shock-Associated Noise with and without Screech," NASA TM-81590, 1980.

[11] Goodykoontz, J. H. and Stone, J. R., "Experimental Study of Coaxial Nozzle Exhaust Noise," AIAA Paper 79-0631, March 1979.

[12] Tanna, H. K., Dean, P. D., and Burrin, R. H., "The Generation and Radiation of Supersonic Jet Noise, Vol. III: Turbulent Mixing Noise Data," Lockheed-Georgia Co., Marietta, Ga., Rept. LG76ER0133, Vol. 3, 1976 (also AD-A032882, AFAPL-TR-76-65, Vol. 3).